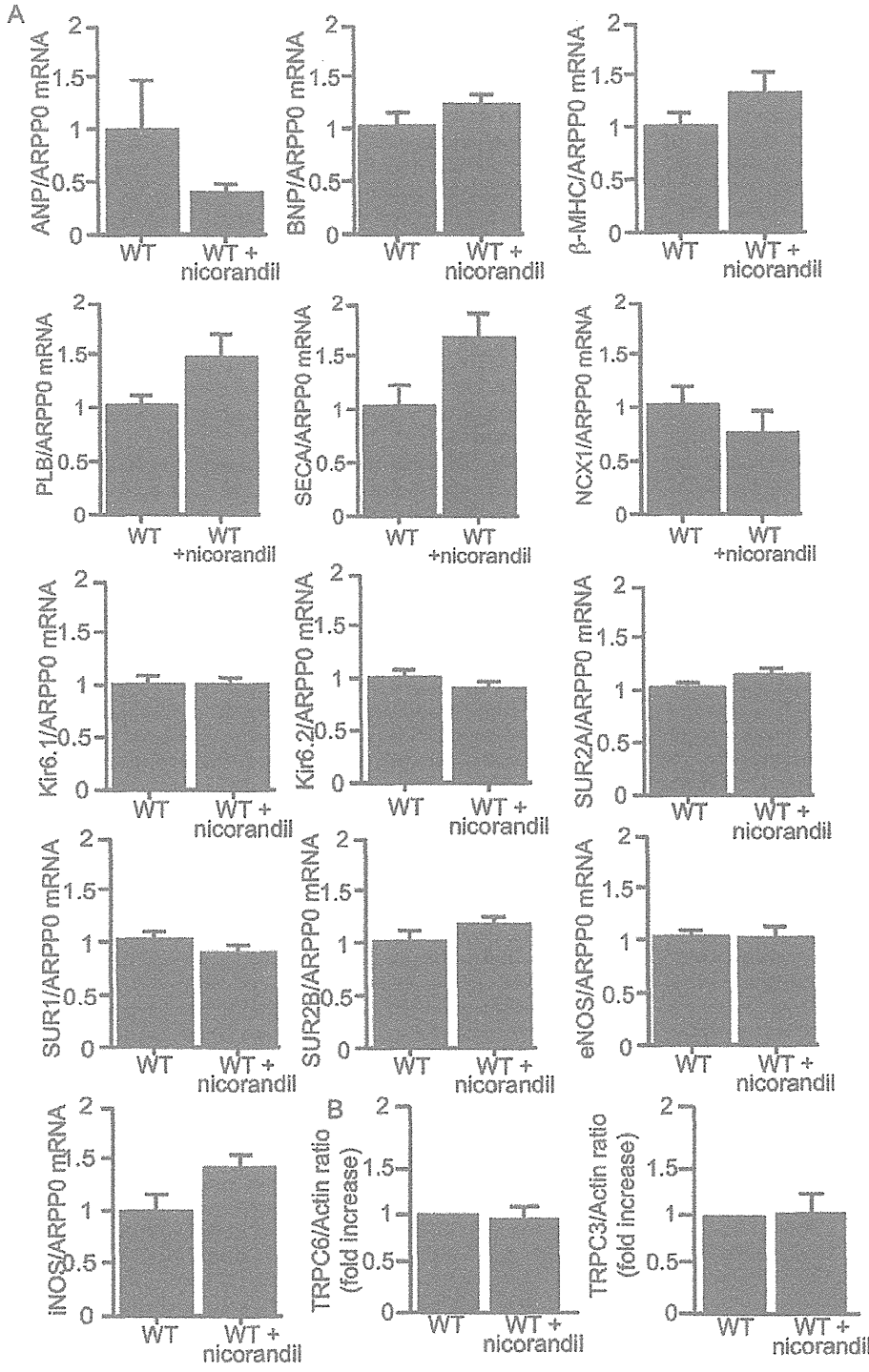

Figure 8. Effects of nicorandil on several gene expressions and on protein expression of TRPC channel isoforms in WT mice. Panel A: Quantitative analyses of ANP, BNP, β-MHC, PLB, SERCA2, NCX1, Kir6.1, Kir6.2, SUR1, SUR2A, SUR2B, eNOS, and iNOS gene expression by real-time RT-PCR in vehicle-treated WT (WT) and nicorandil-treated WT (WT+nicorandil) mouse hearts. The data were normalized to those for ARPP0. Data are the mean ± SE obtained from 5 mice for each group. Panel B: Expression of TRPC channel isoforms in WT+vehicle and WT+nicorandil hearts. TRPC isoform expression was normalized to actin expression and expressed relative to wt (set at 1). Data are the mean ± SE obtained from 5 mice for each group. Mice at the age of 32 weeks were used.
doi:10.1371/journal.pone.0052667.g008

example, intracoronary infusion of acetylcholine normally dilates the conductance and resistance vessels, and this vasodilatation is mediated by the release of endothelium-dependent relaxing factors/nitric oxide (NO). In patients with heart failure, intracoronary infusion of acetylcholine increases coronary artery resistance and decreases coronary blood flow [20]. Therefore, the decreased coronary blood flow reserve with a concurrent increase in myocardial oxygen demand might induce myocardial ischemia, myocyte necrosis and apoptosis in heart failure. Nicorandil is a K_{ATP} channel opener and a nitric oxide donor and widely used as a coronary vasodilator. K_{ATP} channels are comprised of a pore-forming subunit (Kir6.1 or Kir6.2) and a regulatory subunit, sulfonylurea receptors (SUR1 or SUR2). K_{ATP} channels with different combinations of these subunits exist in various tissues and regulate cellular functions, but the combination of Kir6.1 and SUR2B is mainly present in vascular smooth muscle including coronary artery [21]. Nicorandil more selectively activates K_{ATP} channels composed of Kir6.1 and SUR2B. Animal studies have shown that the opening of K_{ATP} channels increases endothelium-derived NO production by eNOS [17], inhibits endothelial cell death [22], and exerts anti-inflammatory [23] and antioxidative effects [24]. These findings suggest that improved endothelial function, anti-inflammatory effects, and reduced oxidative stress may all contribute to the long-term improvement of cardiovascular outcomes seen with nicorandil therapy. In this study, SUR2B gene expression was improved in nicorandil-treated $G\alpha_q$-TG mouse hearts. Moreover, Nicorandil attenuated or prevented the decrease of eNOS in $G\alpha_q$-TG hearts, suggesting that nicorandil improves coronary vasodilatation in this model. Nicorandil may also contribute to a potential upregulation of VEGF expression because deficiency of eNOS resulted in marked impairment of myocardial capillary development and the associated reduction in VEGF expression in the neonatal mouse myocardium [25]. These effects may also contribute to nicorandil-induced improvement of the coronary circulation. Nicorandil prevented decreases in SERCA2 in $G\alpha_q$-TG mouse hearts. It is well known that decreased SERCA2 gene and protein expression causes an abnormal contractile function in failing hearts. Moreover, Koitabashi et al. [26] have suggested that carvedilol restores SERCA2 gene expression through prevention of oxidative stress-mediated downregulation of SERCA2 gene transcription, leading to the improvement of cardiac contractile function in failing hearts. Therefore, nicorandil may improve cardiac contractile function through the normalization of SERCA2 gene expression. In this study, nicorandil failed to improve the increased mRNA expression of profibrotic genes such as CTGF and collagen type 1, suggesting that nicorandil has no effect on the production of those proteins, although whether such protein expression in $G\alpha_q$-TG mice increases or not is still unknown. Nevertheless, nicorandil administration inhibited the increased ventricular interstitial fibrosis. Nicorandil improved the decreased SUR2B and eNOS gene expression in $G\alpha_q$-TG mouse hearts, which may contribute to the inhibition of the ventricular interstitial fibrosis because a previous study has demonstrated that nicorandil inhibits cardiac fibroblast proliferation induced by angiotensin II by activating K_{ATP} channels and the eNOS-NO pathway [27]. Therefore, nicorandil-induced coronary vasodilatation, upregulation of VEGF expression, improvement of SERCA2 gene expression, and inhibition of ventricular interstitial fibrosis might prevent the progression of heart failure. NO donors are commonly used in the management of patients with HF. However, the relevant clinical data do not manifest the broad beneficial effects observed in the present study with nicorandil. Moreover, a previous study has demonstrated that SUR2B immunoreactivity mainly occurred in the mitochondria as well as in the endoplasmic reticulum and cell membrane [28]. Thus, in this transgenic model of HF, the activation of K_{ATP} channels including that in the mitochondria may play an important mechanistic role in the beneficiary effects of nicorandil. In this study, we found that chronic nicorandil administration shortened the prolonged QT interval and reduced ventricular arrhythmias such as PVC in $G\alpha_q$-TG mice. Numerous studies have characterized the ionic and molecular remodeling that occurs in the failing heart. One major change in the failing heart is a prolonged action potential duration which is linked mainly to downregulation of repolarizing potassium currents and an increase in late sodium current density [29]. HF-induced prolongation of action potential predisposes one to $I_{Ca\text{-}L}$ reactivation underlying the generation of early after depolarization (EAD), which can act as initiating triggers for ventricular arrhythmias in HF. These results suggest that prevention of the progression of HF by chronic nicorandil treatment helps to prevent ventricular arrhythmias by shortening the prolonged QT interval in this model.

In this study, we found that acute nicorandil administration shortened ventricular monophasic action potential duration in Langendorff-perfused $G\alpha_q$-TG hearts and reduced the number of PVCs. As described above, HF-induced action potential prolongation predisposes individuals to $I_{Ca\text{-}L}$ reactivation underlying the generation of EAD, which can act as initiating triggers for ventricular arrhythmias in HF. In our previous study, EAD-induced triggered activity was frequently observed in single ventricular myocytes of $G\alpha_q$-TG mice [11]. These results suggest that effects of acute nicorandil administration on ventricular action potential duration contributes to the inhibition of EAD-induced triggered activity and PVCs in $G\alpha_q$-TG mice. Numerous studies have demonstrated that the pore-forming Kir6.2 and regulatory SUR2A subunits are essential elements of the sarcolemmal K_{ATP} channel in ventricular cardiomyocytes of several animals including mice. In this study, Kir6.2 and SUR2A gene expression was decreased in vehicle-treated $G\alpha_q$-TG mouse hearts, and nicorandil did not prevent the decreased expression of these genes. Moreover, nicorandil selectively activates K_{ATP} channels composed of Kir6.1 and SUR2B. Nevertheless, nicorandil shortened the prolonged QT interval and ventricular action potential duration in $G\alpha_q$-TG mouse hearts. In our previous study, we have shown that nicorandil dose-dependently shortened ventricular action potential duration before ischemia and augmented action potential duration shortening without increasing the dispersion of action potential duration during ischemia [6]. These effects of nicorandil were inhibited by HMR1098, suggesting that the activation of sarcolemmal K_{ATP} channels on the ventricular myocytes by nicorandil shortened APD homogenously. Moreover, our previous result suggested that nicorandil activates sarcolemmal K_{ATP} channels in cardiac muscle more effectively in ischemia than non-ischemia [30]. In fact, the present results demonstrated that HMR1098 significantly attenuated the shortening of MAP duration induced by nicorandil in the $G\alpha_q$-TG heart. Therefore, nicorandil may more effectively shorten the prolonged ventricular action potentials in failing hearts in which relative myocardial ischemia might occur. Thus, nicorandil may prevent ventricular arrhythmias not only by preventing progressive HF but also by shortening action potential duration.

Several studies have shown that K_{ATP} channel agonists inhibit the development of cardiac hypertrophy. In fact, nicorandil inhibited cardiac hypertrophy after myocardial infarction through the inhibition of p70S6 kinase [31]. Moreover, a K_{ATP} channel agonist also inhibited the increased cell size in rat heart-derived H9c2 cells [32]. However, chronic administration of nicorandil for

24 weeks failed to inhibit the development of cardiac hypertrophy in $G\alpha_q$-TG mice. It is well known that the development of cardiac hypertrophy is a multigenic, integrative response involving multiple pathways. A recent study has shown that activation of TRPC3 and 6 channels participates in the generation of cardiac hypertrophy [16]. Our previous study demonstrated that the protein expression of TRPC3 and 6 was increased in $G\alpha_q$-TG mouse hearts [11]. Moreover, nicorandil did not inhibit the increased expression of TRPC 3 and 6 proteins and of fetal type genes in $G\alpha_q$-TG hearts (Fig. 3). Therefore, the failure to completely abrogate the hypertrophic process was not surprising in view of the underlying complexity of the process.

While vehicle-treated $G\alpha_q$-TG mice age-dependently exhibited reduced left ventricular contractility and chamber dilation between 8 and 32 weeks of age, nicorandil-treated $G\alpha_q$-TG mice did not. Moreover, a previous study demonstrated that in $G\alpha_q$-TG mice LVFS was decreased by approximately 27% at the age of 16 weeks similar to that at the age of 32 weeks in this study [10]. These results suggest that nicorandil prevents age-dependent progression of cardiomegaly and contractile dysfunction in $G\alpha_q$-TG mice. Thus, the increased expression of eNOS, SUR2B, and SERCA2 mRNA may play important roles in prevention of the progression of heart failure in younger $G\alpha_q$-TG mice.

Supporting Information

Table S1 Primers used in this study.
(XLS)

Acknowledgments

We are grateful to Ms. Reiko Sakai for her secretarial assistance.

Author Contributions

Conceived and designed the experiments: MH YT KM MY. Performed the experiments: MH HS TN TK AN SS NM FS. Analyzed the data: MH HS TN TK SS. Contributed reagents/materials/analysis tools: MH YT UM. Wrote the paper: MH UM MY ET.

References

1. Lefer DJ, Lefer AM (1988) Studies on the mechanism of the vasodilator action of nicorandil. Life Sci 42: 1907–1914.
2. Holzmann S (1983) Cyclic GMP as possible mediator of coronary arterial relaxation by nicorandil. J Cardiovasc Pharmacol 5: 364–370.
3. Noguchi K, Matsuzaki T, Ojiri Y, Koyama T, Nakasone J, et al. (1998) Beneficial hemodynamic effects of nicorandil in a canine model of acute congestive heart failure: comparison with nitroglycerin and cromakalim. Fundam Clin Pharmacol 12: 270–278.
4. Izawa H, Iwase M, Takeichi Y, Somura F, Nagata K, et al. (2003) Effect of nicorandil on left ventricular end-diastolic pressure during exercise in patients with hypertrophic cardiomyopathy. Eur Heart J 24: 1340–1348.
5. Xu J, Nagata K, Obata K, Ichihara S, Izawa H, et al. (2005) Nicorandil promotes myocardial capillary and arteriolar growth in the failing heart of Dahl salt-sensitive hypertensive rats. Hypertension 46: 719–724.
6. Hirose M, Tsujino N, Nakada T, Yano S, Imamura H, et al. (2008) Mechanisms of preventive effect of nicorandil on ischemia-induced ventricular tachyarrhythmia in isolated arterially perfused canine left ventricular wedges. Basic & Clinical Pharmacol Toxicol 102: 504–514.
7. Bogoyevitch MA, Sugden PH (1996) The role of protein kinases in adaptational growth of the heart. Int J Biochem Cell Biol 28: 1–12.
8. Hunter JJ, Chien KR (1999) Signaling pathways for cardiac hypertrophy and failure. N Engl J Med 341: 1276–1283.
9. Takeishi Y, Jalili T, Ball NA, Walsh RA (1999) Responses of cardiac protein kinase C isoforms to distinct pathological stimuli are differentially regulated. Circ Res 85: 264–271.
10. Niizeki T, Takeishi Y, Kitahara T, Arimoto T, Koyama Y, et al. (2008) Diacylglycerol kinase zeta rescues G alpha q-induced heart failure in transgenic mice. Circ J 72: 309–317.
11. Hirose M, Takeishi Y, Niizeki T, Nakada T, Shimojo H, et al. (2011) Diacylglycerol kinase ε inhibits ventricular tachyarrhythmias in a mouse model of heart failure: Roles of canonical transient receptor potential (TRPC) channels. Circ J 75: 2333–2342.
12. Mende U, Kagen A, Cohen A, Aramburu J, Schoen FJ, et al. (1998) Transient cardiac expression of constitutively active Gαq leads to hypertrophy and dilated cardiomyopathy by calcineurin-dependent and independent pathways. Proc Natl Acad Sci USA 95: 13893–13898.
13. Kamiyoshi Y, Takahashi M, Yokoseki O, Yazaki Y, Hirose S, et al. (2005) Mycophenolate mofetil prevents the development of experimental autoimmune myocarditis. J Mol Cell Cardiol 39: 467–477.
14. Hirose M, Takeishi Y, Niizeki T, Shimojo H, Nakada T, et al. (2009) Diacylglycerol kinase ζ inhibits Gαq-induced atrial remodeling in transgenic mice. Heart Rhythm 6: 78–84.
15. Niizeki T, Takeishi Y, Kitahara T, Arimoto T, Ishino M, et al. (2008) Diacylglycerol kinase-ε restores cardiac dysfunction under chronic pressure overload: a new specific regulator of Gαq signaling cascade. Am J Physiol 295: H245-H255.
16. Onohara N, Nishida M, Inoue R, Kobayashi H, Sumimoto H, et al. (2006) TRPC3 and TRPC6 are essential for angiotensin II-induced cardiac hypertrophy. EMBO J 25: 5305–5316.
17. Horinaka S, Kobayashi N, Higashi T, Hara K, Hara S, et al. (2001) Nicorandil enhances cardiac endothelial nitric oxide synthase expression via activation of adenosine triphosphate-sensitive K channel in rat. J Cardiovasc Pharmacol 38: 200–210.
18. Treasure CB, Vita JA, Cox DA, Fish RD, Gordon JB, et al. (1990) Endothelium-dependent dilation of the coronary microvasculature is impaired in dilated cardiomyopathy. Circulation 81: 772–779.
19. Coma-Canella I, García-Velloso MJ, Macías A, Villar L, Cosín-Sales J, et al. (2003) Impaired coronary flow reserve in patients with non-ischemic heart failure. Rev Esp Cardiol 56: 354–360.
20. Canetti M, Akhter MW, Lerman A, Karaalp IS, Zell JA, et al. (2003) Evaluation of myocardial blood flow reserve in patients with congestive heart failure due to idiopathic dilated cardiomyopathy. Am J Cardiol 92: 1246–1249.
21. Seino S (1999) ATP-sensitive potassium channels: a model of heteromultimeric potassium channel/receptor assemblies. Annu Rev Physiol 61: 337–362.
22. Date T, Taniguchi I, Inada K, Matsuo S, Miyanaga S, et al. (2005) Nicorandil inhibits serum starvation induced apoptosis in vascular endothelial cells. J Cardiovasc Pharmacol 46: 721–726.
23. Hongo M, Mawatari E, Sakai A, Ruan Z, Koizumi T, et al. (2005) Effects of nicorandil on monocrotalineinduced pulmonary arterial hypertension in rats. J Cardiovasc Pharmacol 46: 452–458.
24. Teshima Y, Akao M, Baumgartner WA, Marbán E (2003) Nicorandil prevents oxidative stress-induced apoptosis in neurons by activating mitochondrial ATP-sensitive potassium channels. Brain Res 990: 45–50.
25. Zhao X, Lu X, Feng Q (2002) Deficiency in endothelial nitric oxide synthase impairs myocardial angiogenesis. Am J Physiol 283: H2371–H2378.
26. Koitabashi N, Arai M, Tomaru K, Takizawa T, Watanabe A, et al. (2005) Carvedilol effectively blocks oxidative stress-mediated downregulation of sarcoplasmic reticulum Ca^{2+}-ATPase 2 gene transcription through modification of Sp1 binding. Biochem Biophys Res Commun 328: 116–124.
27. Liou JY, Hong HJ, Sung LC, Chao HH, Chen PY, et al. (2011) Nicorandil inhibits angiotensin-II-induced proliferation of cultured rat cardiac fibroblasts. Pharmacology 87: 144–151.
28. Zhou M, He HJ, Suzuki R, Liu KX, Tanaka O, et al. (2007) Localization of sulfonylurea receptor subunits, SUR2A and SUR2B, in rat heart. J Histochem Cytochem 55: 795–804.
29. Kaab S, Nuss HB, Chiamvimonvat N, O'Rourke B, Pak PH, et al. (1996) Ionic mechanism of action potential prolongation in ventricular myocytes from dogs with pacing-induced heart failure. Circ Res 78: 262–273.
30. Yamada M, Kurachi Y (2004) The nucleotide-binding domains of sulfonylurea receptor 2A and 2B play different functional roles in nicorandil-induced activation of ATP-sensitive K^+ channels. Mol. Pharmacol 65: 1198–1207.
31. Lee TM, Lin MS, Chang NC (2008) Effect of ATP-sensitive potassium channel agonists on ventricular remodeling in healed rat infarcts. J Am Coll Cardiol 51: 1309–1318.
32. Hwang GS, Oh KS, Koo HN, Seo HW, You KH, et al. (2006) Effects of KR-31378, a novel ATP-sensitive potassium channel activator, on hypertrophy of H9c2 cells and on cardiac dysfunction in rats with congestive heart failure. Eur J Pharmacol 540: 131–138.

EDITORIAL COMMENTARY

A new therapeutic approach for postoperative systemic inflammation: Effectiveness of epicardial ganglionated plexus stimulation

Masamichi Hirose, MD, PhD,* Naoko Matsushita, MD†

*From the *Department of Molecular and Cellular Pharmacology, School of Pharmaceutical Sciences, and †Department of Pharmacology, School of Medicine, Iwate Medical University, Iwate, Japan.*

There is great interest in developing novel therapeutic approaches that target the inhibition of systemic inflammation after cardiac surgery. It is well known that postoperative systemic inflammation plays a prominent role in the induction of organ dysfunction and postoperative complications, especially postoperative atrial fibrillation.[1] Several therapeutic approaches have been developed to inhibit postoperative systemic inflammation, leading to the inhibition of postoperative atrial fibrillation. Drugs such as corticosteroids and statins have been used to inhibit postoperative systemic inflammation and atrial fibrillation.[2–4] Recently, implantable medical devices are being increasingly used in the treatment of several diseases traditionally targeted with drugs. In fact, recent experimental data using animal models support the rationale for, and feasibility of, developing implantable vagal nerve stimulation devices to treat inflammation in humans because stimulation of the cholinergic antinflammatory pathway by electrical stimulation of the vagal nerve can inhibit systemic inflammation.[5,6] In this issue of Heart*Rhythm*, Rossi et al[7] present the results of an interesting study on the potential therapeutic approach of electrical stimulation of intrinsic cardiac autonomic nerves using an implantable medical device in the inhibition of systemic inflammation after off-pump coronary artery bypass graft (CABG). They clearly demonstrate that postoperative electrical stimulation of the inferior vena cava-inferior atrial ganglionated plexus (IVC-IAGP) significantly decreases the serum levels of inflammatory cytokines such as IL-6, TNF-α, vascular endothelial growth factor, and epidermal growth factor, suggesting the inhibition of systemic inflammation after off-pump CABG. They also show that prolonged burst electrical stimulation of IVC-IAGP after the surgery appears feasible and safe.

This study is of marked interest for a variety of reasons. First, this article demonstrates that a part of intrinsic cardiac autonomic nerve stimulation (ie, IVC-IAGP stimulation) inhibits serum levels of proinflammatory cytokines as a marker of systemic inflammation. In fact, numerous studies have demonstrated that cervical vagal nerve stimulation can induce antisystemic inflammatory responses.[5,6] Interestingly, a recent study on the cholinergic anti-inflammatory pathway indicated that the spleen is required for vagal nerve control of inflammation.[8] The spleen is a major source of serum TNF during endotoxemia.[8,9] Splenectomy reduces serum TNF by 70%, and vagal nerve stimulation fails to further suppress TNF in endotoxin-treated rats. Moreover, vagal nerve stimulation attenuates TNF mRNA and protein levels in the spleen, and selective surgical ablation of the common celiac vagal branches prevents TNF inhibition by electrical stimulation of the vagal nerves.[8] In contrast to cervical vagal stimulation, cardiac vagal nerve stimulation directly reduces the myocardial damage induced by ischemia reperfusion injury through the upregulation of myocardial energy consumption, anti–apoptosis-related protein stimulation, and the inhibition of mitochondrial swelling,[10] whereas it increases the expression levels of TNF-α in cardiomyocytes.[11] Therefore, the present study provides an interesting insight into the possibility of a new therapeutic approach using the intrinsic cardiac autonomic nervous system for the inhibition of postoperative systemic inflammation after off-pump CABG. Second, this small clinical study also provides an interesting insight into the relationship between epicardial ganglionated plexus (GP) stimulation and postoperative atrial fibrillation, which is one of the most frequent complications of cardiac surgery and an important predictor of patient morbidity as well as of prolonged hospitalization. It is known that epicardial GP ablation, a common part of surgical atrial fibrillation ablation, has been shown to be effective in treating atrial fibrillation,[12] suggesting that postoperative atrial fibrillation is worse for epicardial GP stimulation. However, the present study showed that although the number of patients enrolled was not large enough to reach significance, IVC-IAGP stimulation, one of the epicardial GPs, tended to decrease the incidence of postoperative atrial fibrillation (25% for the

Address for reprint requests and correspondence: Dr Masamichi Hirose, MD, PhD, Department of Molecular and Cellular Pharmacology, School of Pharmaceutical Sciences, Iwate Medical University, Shiwa-gun, Iwate 028-3694, Japan. E-mail address: mhirose@iwate-med.ac.jp.

http://dx.doi.org/10.1016/j.hrthm.2012.03.004

control group vs 7% for the IVC-IAGP stimulation group). This result seems to suggest the preventive effect of GP stimulation on postoperative atrial fibrillation. A previous study that demonstrated that the preservation of the anterior fat pad decreases the incidence of postoperative atrial fibrillation after cardiac surgery[13] may support the present results. Clinical studies indicate that the main pathophysiological factors inducing postoperative atrial fibrillation after off-pump CABG are inflammation[14] and sympathetic activation, especially beta-adrenergic activation.[15] In the present study, GP stimulation significantly decreased the serum levels of inflammatory cytokines as a parameter of inflammation after off-pump CABG, expecting the stimulation to inhibit postoperative atrial fibrillation. Moreover, it is possible that GP stimulation decreases the increased sympathetic activity through a mechanism of accentuated antagonism,[16] which may contribute to the inhibition of postoperative atrial fibrillation. However, GP stimulation with the increased sympathetic activity also induces atrial tachyarrhythmias.[17] Either way, it will be important to clarify the effectiveness of epicardial GP stimulation in the inhibition of postoperative atrial fibrillation after cardiac surgery including off-pump CABG through a large randomized clinical trial.

Like all important findings, this one raises a variety of questions. The most important question is whether this GP stimulation therapy using an implantable medical device is as effective and safe as or more effective and safer than pharmacological therapy in reducing the induction of organ dysfunction and postoperative complications such as atrial fibrillation after cardiac surgery. Corticosteroids reduce the incidence of new-onset postoperative atrial fibrillation by inhibiting proinflammatory cytokine release and the duration of mechanical ventilation but with fewer potential side effects after coronary surgery.[2] Moreover, preoperative statin therapy decreases inflammation markers[3] and reduces postoperative complications such as postoperative atrial fibrillation,[4] whereas it is also associated with a significantly higher incidence of postoperative atrial fibrillation compared with no statin treatment in patients undergoing isolated CABG.[18] Therefore, it is hoped that this therapy will become a new modality to effectively inhibit the induction of organ dysfunction and postoperative complications. This study demonstrated that epicardial GP stimulation for 6 hours decreased proinflammatory cytokines but did not significantly reduce the incidence of postoperative atrial fibrillation. Postoperative atrial fibrillation mostly develops between 48 and 72 hours after surgery.[19] Thus, a question still remains about the optimum periods for the electrical stimulation of intrinsic cardiac autonomic nerves to inhibit postoperative atrial fibrillation. It will also be important to determine whether prolonged burst electrical stimulation of IVC-IAGP for more than 6 hours is feasible and safe and whether the electrical stimulation of an epicardial GP different from IVC-IAGP is effective. Moreover, although GP stimulation is an attractive therapeutic target for the inhibition of postoperative complications, a better understanding of the underlying mechanisms is needed in order to develop more rationally based treatment approaches. The development of a new therapeutic approach by Rossi et al merits further study on the inhibition of the induction of organ dysfunction and postoperative complications such as atrial fibrillation after cardiac surgery.

References

1. Hill GE. Cardiopulmonary bypass-induced inflammation: is it important? J Cardiothorac Vasc Anesth 1998;12:21–25.
2. Ho KM, Tan JA. Benefits and risks of corticosteroid prophylaxis in adult cardiac surgery: a dose-response meta-analysis. Circulation 2009;119:1853–1866.
3. Chello M, Anselmi A, Spadaccio C, et al. Simvastatin increases neutrophil apoptosis and reduces inflammatory reaction after coronary surgery. Ann Thorac Surg 2007;83:1374–1380.
4. Mariscalco G, Lorusso R, Klersy C, et al. Observational study on the beneficial effect of preoperative statins in reducing atrial fibrillation after coronary surgery. Ann Thorac Surg 2007;84:1158–1164.
5. Bernik TR, Friedman SG, Ochani M, et al. Cholinergic antiinflammatory pathway inhibition of tumor necrosis factor during ischemia reperfusion. J Vasc Surg 2002;36:1231–1236.
6. Bernik TR, Friedman SG, Ochani M, et al. Pharmacological stimulation of the cholinergic antiinflammatory pathway. J Exp Med 2002;195:781–788.
7. Rossi P, Ricci A, De Paulis R, et al. Epicardial ganglionated plexus stimulation decreases postoperative inflammatory response in humans. Heart Rhythm 2012; 9:943–950.
8. Huston JM, Ochani M, Rosas-Ballina M, et al. Splenectomy inactivates the cholinergic antiinflammatory pathway during lethal endotoxemia and polymicrobial sepsis. J Exp Med 2006;203:1623–1628.
9. Mignini F, Streccioni V, Amenta F. Autonomic innervation of immune organs and neuroimmune modulation. Auton Autacoid Pharmacol 2003;23:1–25.
10. Katare RG, Ando M, Kakinuma Y, et al. Vagal nerve stimulation prevents reperfusion injury through inhibition of opening of mitochondrial permeability transition pore independent of the bradycardiac effect. J Thorac Cardiovasc Surg 2009;137:223–231.
11. Katare RG, Ando M, Kakinuma Y, Arikawa M, Yamasaki F, Sato T. Differential regulation of TNF receptors by vagal nerve stimulation protects heart against acute ischemic injury. J Mol Cell Cardiol 2010;49:234–244.
12. Nakagawa H, Scherlag BJ, Patterson E, Ikeda A, Lockwood D, Jackman WM. Pathophysiologic basis of autonomic ganglionated plexus ablation in patients with atrial fibrillation. Heart Rhythm 2009;6:S26–S34.
13. Cummings JE, Gill I, Akhrass R, Dery M, Biblo LA, Quan KJ. Preservation of the anterior fat pad paradoxically decreases the incidence of postoperative atrial fibrillation in humans. J Am Coll Cardiol 2004;43:994–1000.
14. Ishida K, Kimura F, Imamaki M, et al. Relation of inflammatory cytokines to atrial fibrillation after off-pump coronary artery bypass grafting. Eur J Cardiothorac Surg 2006;29:501–505.
15. Kalisnik JM, Avbelj V, Trobec R, et al. Assessment of cardiac autonomic regulation and ventricular repolarization after off-pump coronary artery bypass grafting. Heart Surg Forum 2006;9:E661–E667.
16. Levy MN. Sympathetic-parasympathetic interactions in the heart. Circulation 1971;29:437–445.
17. Hirose M, Imamura H. Mechanisms of atrial tachyarrhythmia induction in a canine model of autonomic tone fluctuation. Basic Res Cardiol 2007;102:52–62.
18. Miceli A, Fino C, Fiorani B, et al. Effects of preoperative statin treatment on the incidence of postoperative atrial fibrillation in patients undergoing coronary artery bypass grafting. Ann Thorac Surg 2009;87:1853–1858.
19. Hogue CW Jr, Hyder ML. Atrial fibrillation after cardiac operation: risks, mechanisms, and treatment. Ann Thorac Surg 2000;69:300–306.

Am J Physiol Heart Circ Physiol 302: H1645–H1654, 2012.
First published February 3, 2012; doi:10.1152/ajpheart.00589.2011.

Chronic receptor-mediated activation of $G_{i/o}$ proteins alters basal t-tubular and sarcolemmal L-type Ca^{2+} channel activity through phosphatases in heart failure

Toshihide Kashihara,[1] Tsutomu Nakada,[1] Hisashi Shimojo,[2] Miwa Horiuchi-Hirose,[1] Simmon Gomi,[1,3] Toshihide Shibazaki,[1,4] Xiaona Sheng,[1,5] Masamichi Hirose,[6] Minoru Hongo,[7] and Mitsuhiko Yamada[1]

[1]Departments of Molecular Pharmacology, [2]Pathology, and [3]Cardiovascular Medicine, Shinshu University School of Medicine, Nagano; [4]Discovery Research Laboratory II, Research and Development, Kissei Pharmaceutical Company, Limited, Azumino, Nagano; [5]Department of Metabolic Regulation, Institute on Aging and Adaptation, Shinshu University Graduate School of Medicine, Nagano; [6]Department of Molecular and Cellular Pharmacology, School of Pharmaceutical Sciences, Iwate Medical University, Iwate; and [7]Department of Cardiovascular Medicine, Shinshu University School of Health Science, Nagano, Japan

Submitted 14 June 2011; accepted in final form 30 January 2012

Kashihara T, Nakada T, Shimojo H, Horiuchi-Hirose M, Gomi S, Shibazaki T, Sheng X, Hirose M, Hongo M, Yamada M. Chronic receptor-mediated activation of $G_{i/o}$ proteins alters basal t-tubular and sarcolemmal L-type Ca^{2+} channel activity through phosphatases in heart failure. *Am J Physiol Heart Circ Physiol* 302: H1645–H1654, 2012. First published February 3, 2012; doi:10.1152/ajpheart.00589.2011.—L-type Ca^{2+} channels (LTCCs) play an essential role in the excitation-contraction coupling of ventricular myocytes. We previously found that t-tubular (TT) LTCC current density was halved by the activation of protein phosphatase (PP)1 and/or PP2A, whereas surface sarcolemmal (SS) LTCC current density was increased by the inhibition of PP1 and/or PP2A activity in failing ventricular myocytes of mice chronically treated with isoproterenol (ISO mice). In the present study, we examined the possible involvement of inhibitory heterotrimeric G proteins ($G_{i/o}$) in these abnormalities by chronically administrating pertussis toxin (PTX) to ISO mice (ISO + PTX mice). Compared with ISO mice, ISO + PTX mice exhibited significantly higher fractional shortening of the left ventricle. The expression level of $G\alpha_{i2}$ proteins was not altered by the treatment of mice with ISO and/or PTX. ISO + PTX myocytes had normal TT and SS LTCC current densities because they had higher and lower availability and/or open probability of TT and SS LTCCs than ISO myocytes, respectively. A selective PKA inhibitor, H-89, did not affect LTCC current densities in ISO + PTX myocytes. A selective PP2A inhibitor, fostriecin, did not affect SS or TT current density in control or ISO + PTX myocytes but significantly increased TT but not SS LTCC current density in ISO myocytes. These results indicate that chronic receptor-mediated activation of $G_{i/o}$ in vivo decreases basal TT LTCC activity by activating PP2A and increases basal SS LTCC activity by inhibiting PP1 without modulating PKA in heart failure.

t-tubule; protein phosphatase 1; protein phosphatase 2a

HEART FAILURE is one of the leading causes of death in adults in developed nations (3). Even with the recommended medical therapies, the 1-yr mortality rate is >50% in patients with an advanced form of the condition. Thus, further understanding of the pathophysiology of heart failure is necessary to develop novel strategies of medical treatment. Altered Ca^{2+} cycling in cardiac myocytes plays a predominant role in disturbed myocardial function in heart failure (2). In cardiac myocytes, rapid Ca^{2+} influx through L-type Ca^{2+} channels (LTCCs) during action potential opens ryanodine receptors in the sarcoplasmic reticulum to release Ca^{2+} from the sarcoplasmic reticulum [Ca^{2+}-induced Ca^{2+} release (CICR)] (10, 27, 37). CICR in ventricular myocytes takes place mainly at dyads or peripheral junctions where ryanodine receptors on the sarcoplasmic reticulum are closely apposed to LTCCs in t-tubular (TT) or surface sarcolemmal (SS) membranes, respectively (11). In mammalian ventricular myocytes, TT membranes have substantially higher LTCC current density than SS membranes (19) and play an essential role in excitation-contraction (E-C) coupling (30). Thus, it is necessary to measure SS and TT LTCC current density separately to assess alterations in LTCCs under physiological and pathophysiological conditions.

Cardiac E-C coupling is posttranslationally regulated by protein kinases and protein phosphatases (PPs). Phosphorylation of LTCCs by PKA or Ca^{2+}/calmodulin-dependent protein kinase II increases the activity of these channels and augments CICR (27, 35). On the other hand, PP1, PP2A, and PP2B counteract these actions of protein kinases (17). The orchestration of kinases and PPs finely tunes cardiac E-C coupling to provide adequate cardiac output for peripheral metabolic demands under physiological conditions; however, these regulations are often distorted in heart failure. We recently found that in heart failure in mice chronically treated with the β-adrenergic receptor (β-AR) agonist isoproterenol (ISO mice) that abnormality of PP1 and/or PP2A activities causes a decrease in TT LTCC current density and an increase in SS LTCC current density (19). The decrease in TT LTCC current density would contribute to decreased cardiac contractility in heart failure.

In the present study, we sought to identify the intracellular signal transduction system that leads to abnormal LTCC current densities in heart failure. To this end, we paid special attention to the following three lines of evidence. First, PP2A is physically bound to the COOH-terminus of the main $Ca_v1.2$ subunit of LTCCs and locally regulates the phosphorylation of $Ca_v1.2$ subunits (6, 15, 36). Second, heterotrimeric $G_{i/o}$ proteins modulate the activity of PP1/2A in cardiac myocytes (16, 22, 25, 38). Finally, the expression level and/or activity of $G_{i/o}$ often increase in failing cardiac myocytes (9, 29); therefore, we hypothesized that increased activity of $G_{i/o}$ alters LTCC cur-

Address for reprint requests and other correspondence: M. Yamada, Dept. of Molecular Pharmacology, Shinshu Univ. School of Medicine, 3-1-1 Asahi, Matsumoto, Nagano 390-8621, Japan (e-mail: myamada@shinshu-u.ac.jp).

rent density and decreases cardiac contractility via PP1/2A in heart failure.

In the present study, we found, for the first time, that the chronic administration of pertussis toxin (PTX), which selectively inhibits the coupling between G protein-coupled receptors (GPCR) and $G_{i/o}$ proteins, to ISO mice almost completely normalized SS and TT LTCC activity and significantly increased cardiac contractility. PTX increased TT LTCC activity by inhibiting $G_{i/o}$-mediated activation of PP2A and decreased SS LTCC activity by inhibiting $G_{i/o}$-mediated inhibition of PP1 independently of PKA. Thus, we found a novel mechanism by which chronic GPCR-mediated activation of $G_{i/o}$ modulates basal LTCC activity through PPs in failing adult cardiac myocytes.

MATERIALS AND METHODS

Chemicals. Chemicals were purchased from Wako Pure Chemical Industries (Osaka, Japan) unless otherwise indicated. ISO (Sigma-Aldrich, St. Louis, MO) and PTX (Calbiochem, La Jolla, CA) were dissolved in saline. H-89 (Sigma-Aldrich), fostriecin (Calbiochem), and okadaic acid (OA; Calbiochem) were prepared as 1 mmol/l stock solutions in 100% DMSO. Bay K8644 (Sigma-Aldrich) was prepared as 3 mmol/l stock solutions in 100% DMSO. These stock solutions were kept at −20°C until use. When H-89, fostriecin, and OA were used in experiments, the final concentrations of these drugs were extracellularly applied to myocytes at least 30 min before LTCC currents were measured. In experiments with detubulated myocytes, these drugs were applied to myocytes after detubulation. During current measurements, the same concentration of the drugs was continuously applied to myocytes through pipette solution. Bay K8644 was extracellularly applied to myocytes during patch-clamp experiments. The final DMSO concentration of 0.1% did not significantly affect LTCC currents.

Animal model. This investigation conformed with the National Institutes of Health (NIH) *Guide for the Care and Use of Laboratory Animals* (NIH Pub. No. 85-23, Revised 1996). All experiments were carried out in accordance with the Guidelines for Animal Experimentation of Shinshu University and approved by the Committee for Animal Experimentation. Male C57BL/6 adult mice (8–10 wk) were purchased from Japan SLC (Hamamatsu, Shizuoka, Japan). Cardiac hypertrophy and failure were induced in the mice by the subcutaneous injection of 6 mg/kg ISO once daily for 21 days (ISO mice), as previously described (19). Age-matched normal control mice received the same volume of saline only. Different groups of mice were treated with subcutaneous saline plus 10 μg/kg ip PTX (PTX mice) (13) or 6 mg/kg sc ISO plus 10 μg/kg ip PTX (ISO + PTX mice) once daily for 21 days. Animals were used for experiments at least 24 h after the last injection. Animals were euthanized by pentobarbital sodium (30 mg/kg) anesthesia administrated intraperitoneally. The heart was excised from the animals, rinsed in ice-cold modified Tyrode solution containing (in mmol/l) 136.5 NaCl, 5.4 KCl, 1.8 $CaCl_2$, 0.53 $MgCl_2$, 5.5 HEPES, and 5.5 glucose (pH 7.4 with NaOH), and weighed. The heart weight (HW; in mg) was normalized to the body weight (BW; in g) (i.e., HW/BW). Because the BW of ISO and ISO + PTX mice was significantly higher than that of control or PTX mice, HW was also normalized to the tibial length (TL; in mm), which was not significantly different among the four groups of mice (i.e., HW/TL).

Ultrasound cardiography. Cardiac function was assessed with ultrasound cardiography (GE Yokogawa Medical Systems, Tokyo, Japan) in anesthetized mice as previously described (19). Briefly, hearts were viewed at the level of the papillary muscles in the short axis. In M-mode tracings, the average of three consecutive beats was used to measure the following parameters: left ventricular (LV) end-diastolic diameter (EDD), LV end-systolic diameter (ESD), and fractional shortening (FS), which was calculated as follows: FS = (EDD − ESD)/EDD × 100%.

Gross and histological evaluation of hearts. The morphology of the heart was evaluated as previously described (19). Briefly, hearts were fixed in 20% phosphate-buffered formalin at room temperature for 24 h and cut longitudinally or transversely to obtain four-chamber sections or ventricular cross sections, respectively. The tissues were then embedded in paraffin and cut into 4-μm-thick slices. Histological sections were stained with hematoxylin-eosin and examined with a light microscope (BX-51, Olympus, Tokyo, Japan). Wall thickness and the chamber diameter of the LV were measured with an objective micrometer as the scale on digital microscopic images taken from histological sections.

Assessment of expression of $G\alpha_{i2}$ proteins and PPs. Expression of $G\alpha_{i2}$, PP1, and PP2A proteins in heart lysates was assessed with Western blot analysis as previously described (19). Mouse monoclonal anti-$G\alpha_{i2}$ (1:200, Santa Cruz Biotechnology, Santa Cruz, CA), mouse monoclonal anti-PP1 antibody (1:2,000, Abnova, Taipei, Taiwan), mouse monoclonal anti-PP2A antibody (1:5,000, Abnova), or mouse monoclonal anti-α-tubulin (1:3,000, Sigma-Aldrich) was used as the primary antibody. Horseradish peroxidase-conjugated donkey anti-mouse IgG (1:30,000, Jackson ImmunoResearch Laboratories, West Grove, PA) was used as the secondary antibody. Signal intensities of bands were quantified with the Gel analysis program of ImageJ software (NIH, Bethesda, MD).

Isolation of cardiac myocytes. Ventricular myocytes were enzymatically isolated as previously described (19). Briefly, the heart mounted on the Langendorff apparatus was digested with Ca^{2+}-free Tyrode solution containing 0.80 mg/ml collagenase, 0.06 mg/ml protease (Sigma-Aldrich), 1.20 mg/ml hyaluronidase (Sigma-Aldrich), 0.03 mg/ml DNase I (F. Hoffmann-La Roche, Basel, Switzerland), and 0.50 mg/ml BSA at 37°C for 2 min. Isolated ventricular myocytes were suspended in Ca^{2+}-free Tyrode solution containing 1 mg/ml BSA at room temperature, and the Ca^{2+} concentration was gradually increased to 1.8 mmol/l.

Detubulation. Detubulation of isolated ventricular myocytes was carried out with an osmotic shock as previously described (19). Briefly, myocytes were treated with the modified Tyrode solution containing formamide (1.5 mol/l) for 15 min and returned to the modified Tyrode solution.

Electrophysiology. The current of isolated ventricular myocytes was studied in the whole cell configuration of the patch-clamp technique at 35–37°C with a patch-clamp amplifier (Axopatch 200B, Molecular Devices, Sunnyvale, CA; or EPC 8, HEKA Instruments, Bellmore, NY) as previously described (19). Series resistance was always kept <7 MΩ and routinely compensated with the amplifier by ~75%. This resulted in a voltage drop in series resistance of <3.5 mV in the presence of 2-nA membrane currents. LTCC currents were measured with pipette solution containing (in mmol/l) 90 D-glutamate, 10 *N*-methyl-D(−)-glucamine (NMDG), 5 $MgCl_2$, 20 tetraethylammonium chloride, 10 EGTA, 20 HEPES, and 3 ATP (pH 7.3 with CsOH). The bathing solution contained (in mmol/l) 150 NMDG, 5.4 CsCl, 2 $CaCl_2$, 1.2 $MgCl_2$, 2 4-aminopyridine, 5 HEPES, and 5.5 glucose (pH 7.4 with HCl). The membrane potential was stepped from −90 to −50 mV for 200 sec and then for 500 ms to potentials between −110 and +70 mV with a 10-mV increment every 5 s. LTCC currents were isolated as the current inhibited by Cd^{2+} (100 μmol/l) plus nifedipine (10 μmol/l) (37). The peak amplitude of LTCC currents evoked by the 500-ms test pulse was plotted against the membrane potential.

The relationship between the peak whole cell LTCC current density and the membrane potential was fit with the following equation:

$$D_{WC} = G_{max}\{1/(1 + \exp[(E_{0.5\_Act} - E_m)/k_{Act}])\}(E_m - E_{rev}) \quad (1)$$

where D_{WC} is the peak whole cell current density, G_{max} is the maximum conductance density, $E_{0.5\_Act}$ is the half-maximum activation potential, E_m is the membrane potential, k_{Act} is the slope factor of

activation, and E_{rev} is the apparent reversal potential of LTCC currents. Kinetics of the inactivation of whole cell LTCC currents were assessed with the fraction of LTCC currents remaining 100 ms after depolarization at potentials between −20 and +40 mV.

To assess SS and TT LTCC current densities, the peak LTCC current amplitude at 0 mV and the membrane capacitance were measured in nondetubulated and detubulated myocytes. SS and TT LTCC current densities were calculated from these values as previously described (19). Briefly, the LTCC current density in SS and TT (D_{SS} and D_{TT}, respectively) was calculated with the following equations:

$$D_{SS} = (I_D - \alpha \times I_N)/(C_D - \alpha \times C_N) \quad (2)$$

$$D_{TT} = (I_N - I_D)/(C_N - C_D) \quad (3)$$

where I_N and I_D are the peak LTCC current amplitudes at 0 mV of nondetubulated and detubulated myocytes, respectively; C_N and C_D are the membrane capacitances of nondetubulated and detubulated myocytes, respectively; and α is the fraction of TT membranes remaining in detubulated myocytes. α was estimated as 0.17 from binary image analysis of detubulated myocytes stained with a membrane-staining dye (di-8-ANEPPS). Because nondetubulated and detubulated myocytes were different groups of myocytes, the above calculation was carried out with the mean membrane capacitance and current amplitude of each group. It is ideal to measure the membrane capacitance and current amplitude before and after detubulation in the same cells (21). However, the application of formamide during whole cell patch-clamp experiments almost always (>90%) resulted in immediate and irreversible occlusion of patch pipettes. We succeeded in such experiments in only 4 of 50 trials with control myocytes and found that detubulation decreased the membrane capacitance by 27.2 ± 2.4% from 169.75 ± 9.44 to 123.25 ± 5.69 pF, which was not

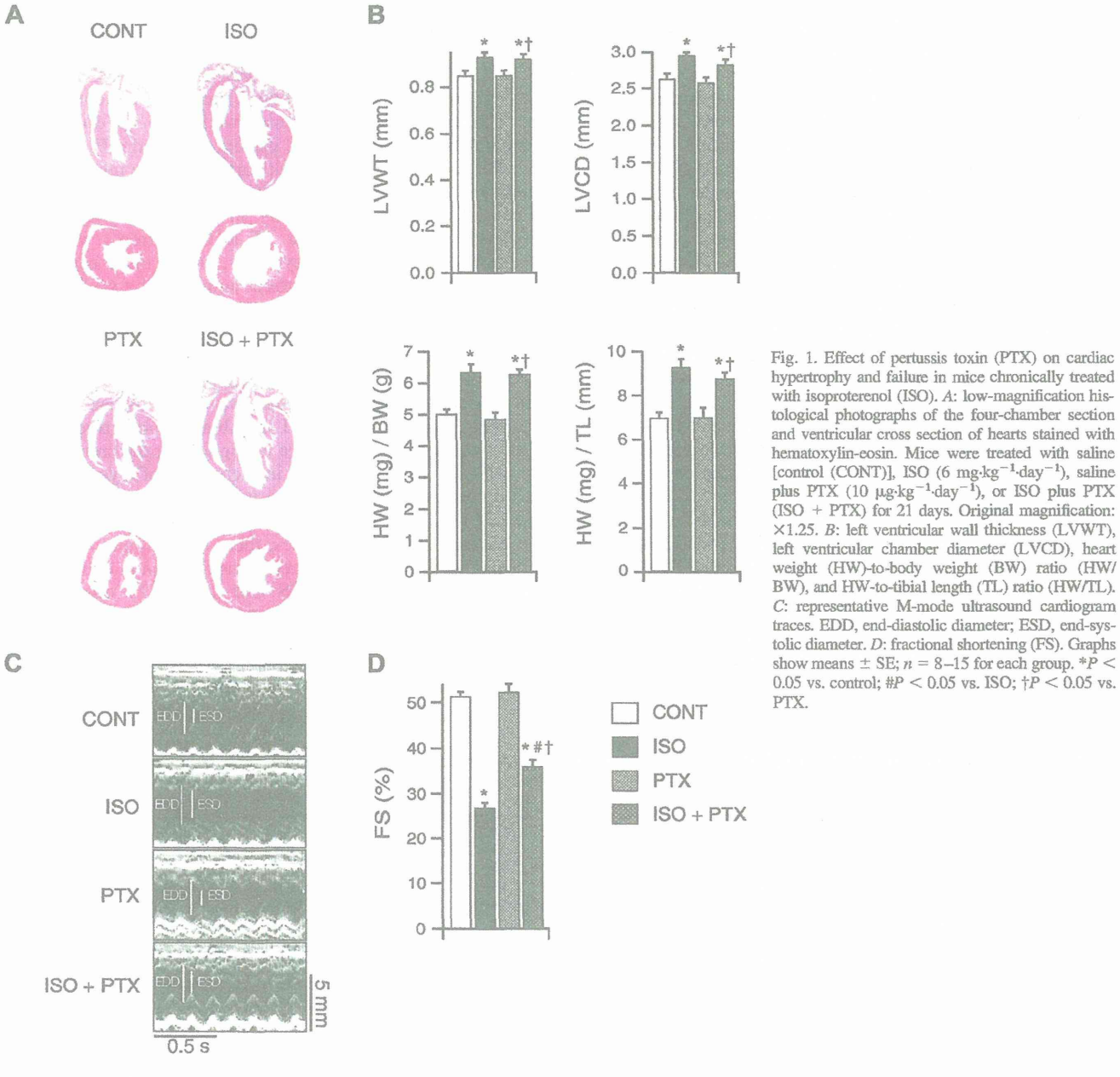

Fig. 1. Effect of pertussis toxin (PTX) on cardiac hypertrophy and failure in mice chronically treated with isoproterenol (ISO). *A*: low-magnification histological photographs of the four-chamber section and ventricular cross section of hearts stained with hematoxylin-eosin. Mice were treated with saline [control (CONT)], ISO (6 mg·kg^{-1}·day^{-1}), saline plus PTX (10 μg·kg^{-1}·day^{-1}), or ISO plus PTX (ISO + PTX) for 21 days. Original magnification: ×1.25. *B*: left ventricular wall thickness (LVWT), left ventricular chamber diameter (LVCD), heart weight (HW)-to-body weight (BW) ratio (HW/BW), and HW-to-tibial length (TL) ratio (HW/TL). *C*: representative M-mode ultrasound cardiogram traces. EDD, end-diastolic diameter; ESD, end-systolic diameter. *D*: fractional shortening (FS). Graphs show means ± SE; n = 8–15 for each group. *P < 0.05 vs. control; #P < 0.05 vs. ISO; †P < 0.05 vs. PTX.

significantly different from the corresponding value assessed in this study (31.9 ± 5.4% from 168.65 ± 4.45 to 114.82 ± 3.02 pF).

The liquid junction potential of the pipette solution in relation to the modified Tyrode solution was −10 mV and taken into consideration throughout this study.

Statistical analysis. Data are shown as means ± SE. Statistical significance was evaluated with Student's unpaired *t*-test. For multiple comparisons of data, ANOVA with Bonferroni's test was used. $P < 0.05$ was considered significant.

RESULTS

Involvement of receptor-mediated activation of $G_{i/o}$ in decreased contractility in mice chronically treated with ISO. We (19) have previously demonstrated that ISO mice showed cardiac hypertrophy and failure compared with saline-treated (control) mice. We first examined whether PTX ameliorated the cardiac hypertrophy and decreased cardiac contractility of ISO mice. Mice were treated with saline alone, ISO alone, saline plus PTX, or ISO plus PTX. ISO and ISO + PTX mice showed cardiac hypertrophy and dilation of chambers compared with control or PTX mice (Fig. 1A). LV wall thickness, LV chamber diameter, HW/BW, and HW/TL were significantly higher in ISO and ISO + PTX mice than control or PTX mice, and these parameters were comparable between ISO and ISO + PTX mice (Fig. 1*B*). Thus, $G_{i/o}$ did not contribute to ISO-induced cardiac hypertrophy. Table 1 shows alterations in the heart rate (HR) and mean systemic blood pressure (MBP) during the treatment of mice with ISO and/or PTX. The HR of ISO mice progressively decreased, probably through the downregulation of β-ARs, whereas that of PTX mice progressively increased through inhibition of $G_{i/o}$. ISO + PTX mice showed HRs between those of ISO and PTX mice. MBP progressively decreased in ISO, PTX, and ISO + PTX mice compared with control mice; however, there was no significant difference in MBP among ISO, PTX, and ISO + PTX mice. M-mode ultrasound cardiogram showed that ISO mice exhibited increased LV EDD and ESD and decreased wall motion compared with control mice, as previously reported (Fig. 1*C*) (19). These parameters of PTX mice were comparable with those of control mice. ISO + PTX mice exhibited smaller LV EDD and ESD and better wall motion than ISO mice. Calculated FS was greatly decreased in ISO versus control mice (Fig. 1*D*). PTX mice had FS comparable with that of control mice. ISO + PTX mice exhibited significantly higher FS than ISO mice. Thus, GPCR-mediated $G_{i/o}$ activation was involved in the decreased cardiac contractility of ISO mice.

Expression levels of $G\alpha_{i2}$ proteins in the heart. The expression level of $G\alpha_{i2}$ proteins often, if not always, increases in different types of heart failure (9, 29). We thus measured the expression level of $G\alpha_{i2}$ proteins, a major PTX substrate in cardiac myocytes. Figure 2 shows Western blot analysis of $G\alpha_{i2}$ proteins. The expression level of $G\alpha_{i2}$ proteins tended to be higher in ISO hearts than in the other hearts, but no significant differences were detected among the four groups of mice.

Effect of PTX on LTCC current density. Because the decreased contractility of ISO mice may result at least partially from decreased TT LTCC density (19), we assessed whether PTX normalized LTCC current density. Figure 3*A* (solid lines) shows representative whole cell LTCC currents of myocytes of each group of mice in response to depolarization to 0 mV from a holding potential of −90 mV. There were no significant differences in peak density, activation or inactivation kinetics, or reversal potential of whole cell LTCC currents among the four groups of myocytes (Table 2). To separately assess SS and TT LTCC current densities, we measured LTCC currents in myocytes with or without detubulation, a procedure to acutely occlude TT in isolated myocytes. As shown in Fig. 3*A* (dotted lines), detubulation reduced LTCC current amplitude. Figure 3*B* shows the pooled data of the peak current-voltage relationships. Detubulation reduced the LTCC current amplitude by 63% in control myocytes but by only 30% in ISO myocytes (Fig. 3, *A* and *B*), indicating that TT LTCC currents were decreased in ISO versus control myocytes. On the other hand, detubulation reduced the LTCC current amplitude by 65% in PTX myocytes and by 62% in ISO + PTX myocytes. Thus, PTX may have increased the decreased TT LTCC current density found in ISO myocytes. From the peak LTCC current amplitude at 0 mV and the membrane capacitance of nondetubulated and detubulated myocytes, we could assess the LTCC current density in SS and TT membrane compartments using *Eqs. 2* and *3* (19). There were no significant differences in whole cell LTCC current density in each group of myocytes (Fig. 3*C*). In control myocytes, there was approximately five times higher LTCC current density in the TT membrane than in the SS membrane. In ISO myocytes, there were significantly higher SS and lower TT LTCC current densities than in control myocytes. PTX myocytes had SS and TT LTCC current densities comparable with those of control myocytes. Notably, ISO + PTX myocytes showed significantly lower SS and higher TT LTCC current densities than ISO myocytes. LTCC current densities in ISO + PTX myocytes were similar to those

Table 1. *Effect of chronic administration of ISO and/or PTX on heart rate and mean systemic blood pressure of mice*

	Control	ISO	PTX	ISO + PTX
Heart rate, beats/min				
Before	636 ± 4	635 ± 21	643 ± 13	627 ± 7
1 wk later	642 ± 6	536 ± 16*	717 ± 11*	613 ± 12†‡
2 wk later	642 ± 9	523 ± 16*	729 ± 12*	607 ± 15†‡
3 wk later	647 ± 9	518 ± 7*	739 ± 5*	599 ± 9*†‡
Mean systemic blood pressure, mmHg				
Before	71.4 ± 1.0	71.4 ± 1.0	71.7 ± 1.9	69.7 ± 1.1
1 wk later	71.1 ± 0.9	63.2 ± 1.2*	68.0 ± 1.6	65.7 ± 0.7*
2 wk later	71.2 ± 1.4	60.5 ± 0.7*	63.7 ± 0.6*	61.6 ± 0.6*
3 wk later	72.1 ± 0.6	60.8 ± 0.1*	62.2 ± 0.3*	60.3 ± 0.3*

Values are means ± SE; $n = 4$ for all groups. ISO, isoproterenol; PTX, pertussis toxin. *$P < 0.05$ vs. control; †$P < 0.05$ vs. ISO; ‡$P < 0.05$ vs. PTX.

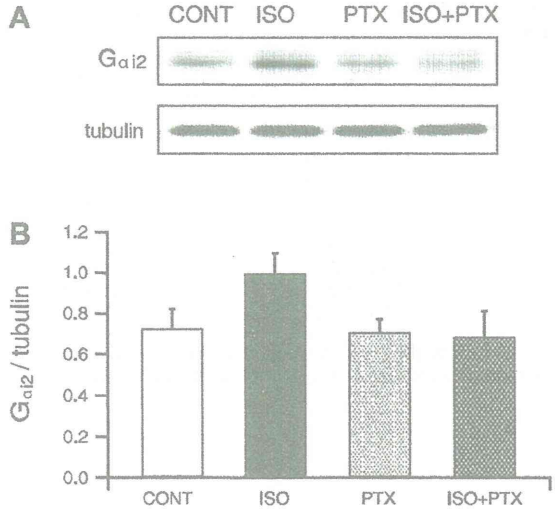

Fig. 2. Expression level of $G_{\alpha i2}$ proteins in the heart. *A*: representative Western blots of $G\alpha_{i2}$ proteins and tubulin. Whole cell fractions of hearts were subjected to SDS-PAGE and immunoblot analysis. *B*: pooled data of the expression level of $G\alpha_{i2}$ proteins normalized to that of tubulin. Graph shows means ± SE; $n = 5$.

of control myocytes; therefore, GPCR-mediated activation of $G_{i/o}$ induced abnormal SS and TT LTCC current densities in ISO myocytes.

Effect of the LTCC agonist Bay K8644 on LTCC density. Next, we examined whether the observed differences in SS and TT LTCC current density among the four groups of myocytes could be ascribed to alteration in the gating and/or expression levels of LTCCs. The density of macroscopic LTCC currents (D) can be described by the following equation: $D = N \times A \times P_o \times i/C_m$, where N is the number of channels, A is the availability, P_o is the open probability, i is the single channel current amplitude, and C_m is the membrane capacitance. The LTCC agonist Bay K8644 (1 μmol/l) almost maximally increases $A \times P_o$ but does not affect other parameters by selectively modulating the gating of LTCCs (18). Figure 4*A* shows SS and TT LTCC current densities in the presence of Bay K8644 (1 μmol/l). Surprisingly, Bay K8644 almost completely abolished the difference in LTCC current density among whole cell, SS, and TT membranes and among the four groups of myocytes. Thus, the observed differences in LTCC density (Fig. 3*C*) seem to be ascribed to a difference in the gating but not the expression level of LTCCs. We also calculated the ratio of LTCC current density in the absence of Bay K8644 to that in the presence of the drug, a parameter reflecting $A \times P_o$ (Fig. 4*B*). The profile of the plot of this parameter closely resembled that of LTCC current density (Fig. 3*C*). Therefore, it is likely that in heart failure, GPCR-mediated activation of $G_{i/o}$ decreased TT LTCC current density and increased SS LTCC current density in ISO myocytes by decreasing or increasing A and/or P_o of LTCCs, respectively.

Effect of a selective PKA inhibitor on the modulation of LTCC current density by PTX. $G_{i/o}$ inhibits adenylyl cyclase (32). Thus, PTX might have increased intracellular cAMP concentration and PKA activity and thereby normalized the TT LTCC activity in ISO + PTX myocytes (27). We thus examined the effect of a selective PKA inhibitor, H-89 (1 μM), on LTCC activity. H-89 did not significantly affect LTCC current densities in control or ISO myocytes, as previously reported (Fig. 5) (19). This indicates that PKA was not activated in these myocytes and that the increased SS LTCC current density in ISO myocytes was not due to the effect of ISO possibly remaining in the preparation of isolated myocytes. H-89 also did not affect LTCC current densities in PTX myocytes, indicating that PTX on its own did not significantly activate PKA. Finally, H-89 did not decrease TT LTCC current density or increase SS LTCC current density in ISO + PTX myocytes. We found that H-89 (10 μmol/l) also did not affect SS or TT LTCC current density in any of the four groups of myocytes

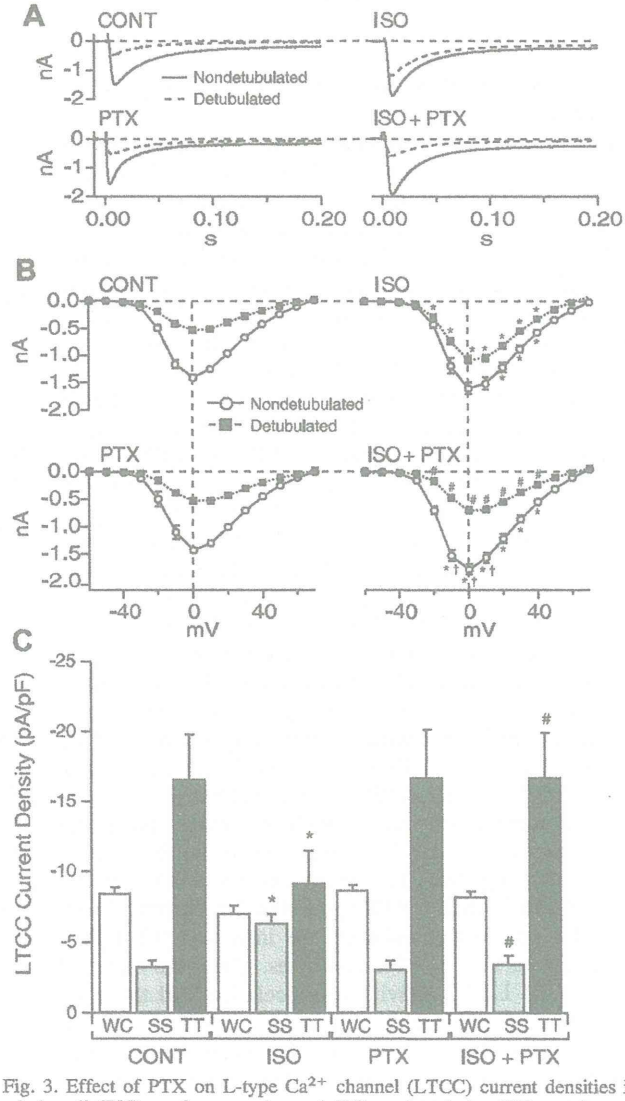

Fig. 3. Effect of PTX on L-type Ca^{2+} channel (LTCC) current densities in whole cell (WC), surface sarcolemmal (SS), and t-tubular (TT) membranes. *A*: representative LTCC currents at 0 mV in control, ISO, PTX, and ISO + PTX myocytes with and without detubulation. *B*: peak current-voltage relationships of LTCC currents in control, ISO, PTX, and ISO + PTX myocytes with and without detubulation. *C*: LTCC current density at 0 mV in WC, SS, and TT membranes in control, ISO, PTX, and ISO + PTX myocytes. Graphs show means ± SE; $n = 6-8$ for each group. *$P < 0.05$ vs. control; #$P < 0.05$ vs. ISO; †$P < 0.05$ vs. PTX.